# Cellular solutions for highly nonequilibrium directional solidification

David A. Kessler

*Department of Physics, University of Michigan, Ann Arbor, Michigan 48109*

Herbert Levine

*Department of Physics and Institute for Nonlinear Science, University of California, San Diego, La Jolla, California 92093*

(Received 18 August 1988)

We compute numerically the cellular shape expected for the directional solidification of CBr$_4$, at velocities far above the threshold for the Mullins-Sekerka instability. Our cell has a smooth tip plunging to a deep narrow channel which ends with a small liquid bubble. Our results are compared to the experimental findings of S. de Cheveigne, C. Guthmann, and M. M. Lebrun [J. Phys. (Paris) **47**, 2095 (1986)].

Solidification patterns are an important class of nonequilibrium structures that can form under the nonlinear dynamics of systems with many degrees of freedom.[1] One such pattern is the periodic cellular array seen when a temperature gradient controls the solidification of a binary compound. This particular structure arises from combination of the tip region dynamics, as it occurs in free growth, and a wavelength selection process, similar to that which occurs in familiar hydrodynamic systems.[2]

There have been several important studies of possible steady-state cellular arrays. Ungar and Brown[3] combined bifurcation analysis with finite element numerical computations to obtain a picture of the solution space near the onset of the Mullins-Sekerka[4] instability. This work has been extended in several directions by other researchers.[5] Dombre and Hakim[6] showed tat one would in general expect a continuous family of solutions (with varying wavelengths), at least for infinite cells in the one-sided limit. This work relies upon an analogy between the tip region of the cell and the Saffman-Taylor finger,[7] pointed out initially by Pelce and Pumir.[8] Their results were verified by the numerical calculations of Ben-Amar and Moussallam.[9] Finally, we have recently shown[10] how to combine all of the above pieces, plus the ideas of "microscopic solvability" as understood for the free growth problem,[1] to form a coherent picture of possible steady patterns from onset all the way to deep cells.

Given our current understanding, the most immediate challenge is to perform a realistic calculation for a given material and experiment. This is what is reported in this work. Our goal is to enable a detailed check of theory by comparison to experimental shapes. This comparison is best done in the simplest possible setting for a system which has the fewest unknown parameters. From our perspective, the experiments of de Cheveigne et al.[11] on CBr$_4$ are quite adequate; for thick enough cells one can use the two-dimensional theory, all the crucial parameters are known, and cell shapes have been determined under well-controlled growth conditions.

Let us briefly review the standard methodology for deriving the boundary integral formulation of directional solidification. We consider a material solidifying in the

presence of a fixed thermal gradient. This geometry allows us to fix an average front velocity. The solidification is diffusion limited, controlled by the release of impurity at the solid-liquid interface. This occurs because of the miscibility gap between the two phases. Under these assumptions, the (normalized) concentration field satisfies the diffusion equation

$$D_{l,s}\nabla^2 C + v\frac{\partial C}{\partial y} = 0 \ ,$$

$$C(y \to \infty) = 1 \ . \tag{1}$$

At the interface,

$$D_l\hat{\mathbf{n}}\cdot\nabla C|_l - D_s\hat{\mathbf{n}}\cdot\nabla C|_s = v_n(C_l - C_s) \ ,$$

$$C_l = \frac{C_s}{k} = -y/l_T - d_0 k \ . \tag{2}$$

Here $k$ is the partition coefficient, and $l_T$, $d_0$ are the thermal and capillary lengths, respectively. We will shortly relate the actual values of all the parameters appearing in these equations.

Let us define a field $C_1$ ($C_2$) which equals $C$ in the liquid (solid) region and is zero elsewhere. This leads to the general representation

$$C_1 = 1 + \int \hat{\mathbf{n}}'\cdot\nabla'G_l C_l + \int G_l \phi_l \ ,$$

$$C_2 = -\int \hat{\mathbf{n}}'\cdot\nabla'G_s C_s + \int G_s \phi_s \ ,$$

where the charge distributions $\phi_l$, $\phi_s$ are unknowns and $G_l$, $G_s$ are the diffusive Green's functions. The Stefan condition requires $\phi_s = \phi_l D_l/D_s \equiv \alpha^{-1}\phi_l$. Evaluating the first (second) equation on the solid (liquid) of the interface we have

$$0 = 1 + \int_{\text{solid}} \hat{\mathbf{n}}'\cdot\nabla'G_l C_l - \int G_l \phi_l \ ,$$

$$0 = -\int_{\text{solid}} \hat{\mathbf{n}}'\cdot\nabla'G_s C_s + \int G_s \alpha^{-1}\phi_l \ . \tag{3}$$

This set of coupled integrodifferential equations enables us to determine both $\phi_l$ and the interface position.

The above equations can be discretized and solved nu-

merically in a straightforward manner; the details of this have been given elsewhere.[10] Here, we just note that the interface is determined by solving for the angle made by the normal vector and $\hat{y}$ axis, $\theta$, at the midpoints of an equal arclength grid running from the tip to the half-wavelength point. Similarly, $\phi_l$ is discretized on the same grid, and the resulting integrals are evaluated by the trapezoidal rule once careful account has been taken of any possible singularities. Once we have reduced the above system to a set of coupled algebraic equations, we can find an exact solution (at fixed $v$) by Newton's algorithm.

At any given set of parameters, solutions are possible for a continuous band of wavelengths. This is in agreement with the results of Dombre and Hakim and Ben-Amar and Moussallam, and has been studied extensively elsewhere. For fixed wavelength there is a discrete set of possible shapes. We will assume that of this discrete set, only the one with the sharpest tip will be linearly stable. This criterion is directly analogous to that proved for Saffman-Taylor fingers and for free dendrites.[12]

The experimental system to be considered is the directional solidification of a thin film of $CBr_4$ with $Br_2$ impurity.[11] The thermal length and capillary length parameters are given by

$$l_T = \frac{MC_\infty}{G} ,$$

$$d_0 = \frac{\sigma(\theta)}{L} \frac{T_M}{MC_\infty} , \quad (4)$$

where $M$ is the liquidus slope, $C_\infty$ the impurity concentration at infinity, $T_M$ the equilibrium melting temperature, $G$ the imposed thermal gradient, $\sigma$ the surface energy, and $L$ the latent heat. A further constant is the crystalline anisotropy $\epsilon$ defined via

$$\sigma(\theta) = \sigma(1 - \epsilon \cos 4\theta) .$$

Choosing to consider the case of $G = 120\,°K/cm$, we find from Table I of de Cheveigne,

$$l_T = 2.9 \times 10^{-3} \text{ cm} ,$$

$$d_0 = 2.13 \times 10^{-5} \text{ cm} .$$

We also need $k = 0.16$ and $D_L = 1.2 \times 10^{-5}$ cm$^{-2}$/sec. The only two unknowns are $\alpha$ and $\epsilon$. We guess that $\epsilon \sim 0.15$, corresponding to a 1% deviation of an equilibrium bubble from a sphere; this is a typical value for plastic crystals.[13] Finally, we do not know $\alpha$, the ratio of solid to liquid diffusivities. We have arbitrarily chosen $\alpha \sim \frac{1}{5}$ but will comment later on the effect of changing the solid diffusivity.

For this choice of parameters, the Mullins-Sekerka instability takes place at around $v = 10$ $\mu$m/sec. For definiteness, we pick $v = 80$ $\mu$m/sec. Our approach is then to generate a solution (using 100 points) at fixed $\lambda$ and then to slowly change $\lambda$ to track the allowed wavelength band. When this is done, there is a maximum wavelength past which solutions cease to exist. For this set of parameters, the maximum value of $p = v\lambda/2D_l$ is approximately $0.56 \pm 0.02$. In physical units, $\lambda_{max} \simeq 35$

$\mu$m. The actual shape of the cell corresponding to this $\lambda$ is shown in Fig. 1. Note the bubble at the bottom, which seems to be a necessary ingredient for obtaining a deep cell solution.

There are several comments in order. First, the shape of the cell in the intermediate region between the tip and the bubble follows the expected Scheil power law.[14] This occurs because the partition coefficient is small and so diffusion into the solid phase is negligible for a relatively long distance away from the tip. Next, this shape evolves continuously from the near-onset shapes studied by Ungar and Brown[3] and others. This is one way of understanding why a continuous band of wavelengths is allowed, since this fact is quite obvious near onset. Finally, the computed shapes vary slowly over the allowed band, if we rescale all our lengths with the wavelength.

As we vary the velocity, the maximum allowed value of the wavelength scales is $v^{-1/2}$. If we assume this dependence, the quantity $\sigma$ defined by

$$\sigma = \frac{2d_0 D}{v(1-k)\lambda^2}$$

is roughly independent of velocity. Using our results at $v = 80$, we find $\sigma \simeq 6 \times 10^{-3}$. This is in rough agreement with the results of wavelength measurements in the $CBr_4$ experiment; their best estimate of this number is $5 \times 10^{-3}$ which corresponds to a wavelength of 30 $\mu$m at $v = 80$. This is quite satisfactory, considering that we have used a rather arbitrary assumption of setting the physical wavelength to the maximum of wavelength of the allowed band. Clearly, a full dynamical theory of wavelength selection (possibly including noise[15]) is necessary before a more detailed wavelength prediction can be made. Once a rescaling to the actual wavelength is carried out, it should be possible to compare the computed cell with the measured one. On a qualitative level, the match appears to be good.

As already mentioned, the solid diffusivity is unknown.
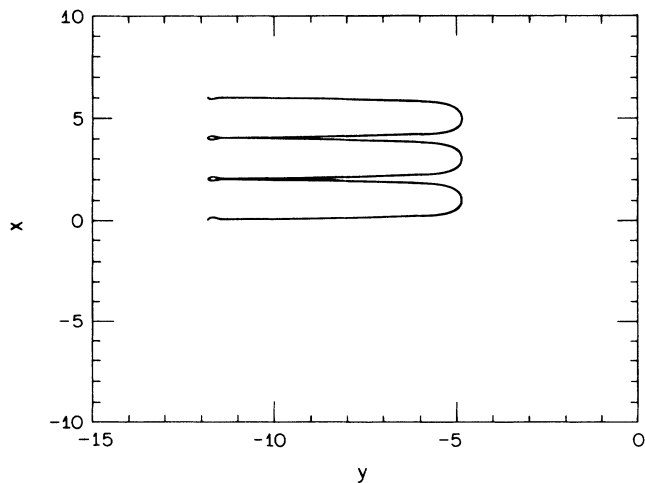


FIG. 1. Cell shape at $v = 80$ $\mu$m/sec, with lengths scaled to half-wavelength.

We have investigated the effect of varying $\alpha$, all other parameters remaining the same. A typical plot of what we can learn is given in Fig. 2. We see that changing $\alpha$ by a factor of 5 has at most a 10% effect on the cell shape. We are therefore confident that should this ratio turn out to be smaller than 0.2, the computed shape will be affected only slightly, presumably becoming slightly deeper. This is consistent with the idea that the most crucial determinant of deep cell structure is the partition coefficient $k$, and not the diffusion constant ratio.

In conclusion, this paper represents an attempt to make a quantitative prediction for a directional solidification pattern from the onset of the Mullins-Sekerka instability. We obtain reasonable agreement with the wavelength seen in the experiments, and our cell shapes are at least qualitatively correct. A more detailed shape comparison should now be possible, with only a slight uncertainty due to unknown material constants, most specifically the solid diffusivity.
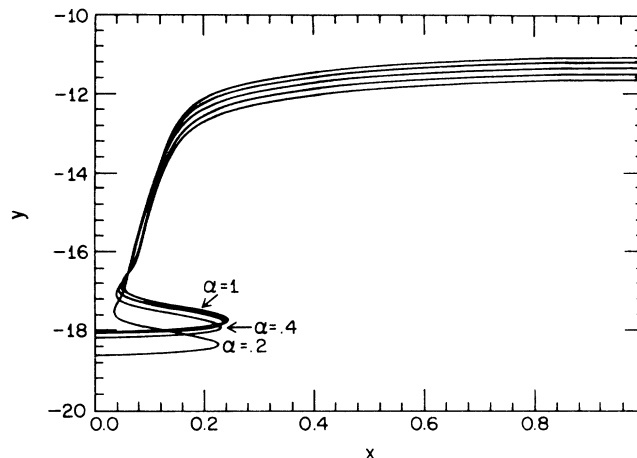


FIG. 2. Dependence of shape on solid to liquid diffusivity ratio $\alpha$.

[1] For recent reviews, see D. Kessler, J. Koplik, and H. Levine, Adv. Phys. 37, 255 (1988); J. Langer, in *Chance and Matter*, edited by J. Souletie et al. (North-Holland, Amsterdam, 1987).

[2] See, for example, *Cellular Structures and Instabilities*, edited by J. E. Wesfried and S. Zaleski (Springer, New York, 1984).

[3] L. H. Ungar and R. A. Brown, Phys. Rev. B 29, 1367 (1984); 30, 3993 (1984); 31, 5923 (1985); 31, 5931 (1985).

[4] W. W. Mullins and R. F. Sekerka, J. Appl. Phys. 34, 323 (1963); 35, 444 (1964).

[5] For the most recent applications of the methods developed in Ref. 3, see G. B. McFadden, R. F. Boisvert, and S. R. Coriell, J. Cryst. Growth 84, 371 (1987); J. D. Hunt and D. G. McCartney, Acta Metall. 35, 89 (1987).

[6] T. Dombre and V. Hakim, Phys. Rev. A 36, 2811 (1987).

[7] J. M. Vanden-Broeck, Phys. Fluids 26, 2033 (1983), and references therein to the original work of Saffman and Taylor.

[8] P. Pelce and A. Pumir, J. Cryst. Growth 73, 337 (1985).

[9] M. Ben-Amar and B. Moussallam, Phys. Rev. Lett. 60, 317 (1988).

[10] D. A. Kessler and H. Levine, Phys. Rev. A 39, 3041 (1988).

[11] S. de Cheveigne, C. Guthmann, and M. M. Lebrun, J. Phys. (Paris) 47, 2095 (1986).

[12] D. A. Kessler and H. Levine, Phys. Rev. A 33, 2621, (1986); 33, 2634 (1986).

[13] For succinonitrile, the best current estimate is 0.75% [M. Glicksman (private communication)].

[14] J. D. Hunt, in *Solidification and Casting of Metals* (The Metals Society, London, 1979).

[15] M. Kerszberg, Phys. Rev. B 27, 3909 (1983); 27, 6796 (1983); Physica 12D, 262 (1984).